ELSEVIER

Journal of Alloys and Compounds 446–447 (2007) 489–494

Journal of ALLOYS AND COMPOUNDS

www.elsevier.com/locate/jallcom

Nuclear magnetic resonance studies of ball-milled hydrides

A.V. Skripov *, A.V. Soloninin, A.L. Buzlukov, A.P. Tankeyev, A.Ye. Yermakov, N.V. Mushnikov, M.A. Uimin, V.S. Gaviko

Institute of Metal Physics, Urals Branch of the Academy of Sciences, S. Kovalevskoi 18, Ekaterinburg 620041, Russia

Received 25 September 2006; received in revised form 14 November 2006; accepted 17 November 2006
Available online 18 December 2006

Abstract

In order to study the effects of mechanical milling on the properties of metal hydrides, we have measured the proton nuclear magnetic resonance (NMR) spectra and spin-lattice relaxation rates in two classes of nanostructured ball-milled systems: Laves-phase hydrides $ZrCr_2H_3$ and MgH_2-based hydrides with some additives (V_2O_5, Al). The proton NMR measurements have been performed at the resonance frequencies of 14, 23.8 and 90 MHz over the temperature range 11–420 K. Hydrogen mobility in the ball-milled $ZrCr_2H_3$ is found to decrease strongly with increasing milling time. The experimental data suggest that this effect is related to the growth of the fraction of highly distorted intergrain regions where H mobility is much lower than in the crystalline grains. For the MgH_2-based systems we have not found any effects of H jump motion at the NMR frequency scale up to 420 K. However, the measured proton spin-lattice relaxation rates for the nanostructured MgH_2-based samples appear to be several orders of magnitude higher than for the coarse-grained MgH_2. This relaxation rate enhancement can be attributed to the interaction between proton spins and intrinsic paramagnetic centers appearing in the process of ball milling.

Keywords: Metal hydrides; Nanostructured materials; Diffusion; Nuclear resonances

1. Introduction

Nanostructured hydrides prepared by ball milling show a number of interesting properties. In particular, the ball milling is known to accelerate the hydrogen absorption/desorption in some hydrogen-storage materials. However, little is known about microscopic mechanisms responsible for the changes in hydrogen reaction kinetics resulting from ball milling. It is of special interest to elucidate the changes in the parameters of hydrogen diffusion in nanostructured hydrides. Nuclear magnetic resonance (NMR) measurements in metal–hydrogen systems can give microscopic information on the hydrogen mobility and hydrogen-induced changes in the electronic structure [1]. Previous applications of NMR to investigation of ball-milled hydrides include the studies of H motion in the ball-milled vanadium–hydrogen [2] and graphite–hydrogen [3] systems. In the present work, the proton NMR is applied to study the behavior of hydrogen in two classes of ball-milled systems: Laves-phase hydrides and Mg-based hydrides.

Laves-phase hydrides AB_2H_x are characterized by rather high volumetric density of hydrogen and high hydrogen mobility [4]. In order to study the effects of ball milling on H mobility in Laves-phase hydrides, we have chosen the cubic (C15-type) system $ZrCr_2H_x$ showing (in the coarse-grained form) the highest H diffusivity [5] at $T < 200$ K among all the studied intermetallic hydrides.

The magnesium dihydride MgH_2 is one of the most attractive materials for hydrogen storage due to its high storage capacity (7.6 wt.% of hydrogen) and low cost of magnesium. However, the kinetics of hydrogen absorption/desorption for Mg is extremely slow. The ball milling of Mg with some additives (such as transition-metal oxides) strongly improves the hydrogenation kinetics [6–8]. While H diffusivity in coarse-grained MgH_2 is known to be very low [9,10], it is not clear whether the mobility of hydrogen becomes significantly higher in nanostructured MgH_2-based systems. In the present work, the emphasis is put on the study of the ball-milled system $MgH_2 + V_2O_5$ showing one of the fastest hydrogenation kinetics in this class of materials.

* Corresponding author. Tel.: +7 343 378 3781; fax: +7 343 374 5244.
E-mail address: skripov@imp.uran.ru (A.V. Skripov).

0925-8388/$ – see front matter © 2006 Elsevier B.V. All rights reserved.
doi:10.1016/j.jallcom.2006.11.091

2. Experimental details

The starting material for preparation of $ZrCr_2$-based hydrides was the powdered $ZrCr_2H_{0.5}$ with the cubic C15-type structure and the lattice parameter $a = 7.278$ Å. This material was placed together with brass balls (powder to ball mass ratio 1:140) into a brass vial. The vial was evacuated and subsequently filled with H_2 gas at a pressure of 110 kPa. The mechanical milling was performed at room temperature using a vibrating ball mill for periods t_m of 1, 3 and 10 h. For all the ball-milled samples, the hydrogen content estimated from the H_2 pressure change in the vial was approximately three H atoms per formula unit of $ZrCr_2$. According to X-ray diffraction analysis, the dominant crystalline phase of the ball-milled samples retained the C15-type structure having the lattice parameters $a = 7.608$ Å ($t_m = 1$ h), 7.645 Å (3 h) and 7.644 Å (10 h). These lattice parameters are close to those found for crystalline $ZrCr_2H_x$ with $x \approx 3$ [11]. However, the diffraction peaks corresponding to the C15-type phase in the ball-milled samples are considerably broader than in the starting material. The average grain size estimated from the peak broadening in the sample with $t_m = 1$ h is 20 nm. The diffraction patterns for the ball-milled samples also contain a minor C15-type phase with $a \approx 7.09$ Å and a very broad amorphous-like feature centered in the angle range of the most intense peaks of the C15-type phase. The intensity of this amorphous-like feature increases with increasing t_m; it becomes the dominant one in the diffraction pattern of the sample with $t_m = 10$ h. This feature can be attributed to highly distorted intergrain regions. In addition to the ball-milled $ZrCr_2H_3$ samples, we have prepared the coarse-grained $ZrCr_2H_3$ by removing hydrogen from $ZrCr_2H_{0.5}$ at high temperature (750 °C) and charging it again to the desired H content. The lattice parameter of the coarse-grained C15-type $ZrCr_2H_3$ is 7.599 Å.

The starting material for preparation of Mg-based hydrides was the magnesium powder with the particle size of 100–200 μm and the purity of 99.8%. The milling of Mg with additives (V_2O_5, Al) in a hydrogen atmosphere was performed in the same way as for $ZrCr_2$-based hydrides. Both steel and brass sets of balls and vial were used. The milling was usually continued until the hydrogen pressure in the vial reached a nearly constant level, typical milling time being about 20 h. According to X-ray diffraction analysis, for all the ball-milled samples the dominant phase was MgH_2 with the average grain size of 12–15 nm. The minor phases were Mg and MgO; in most cases, the additives could not be detected in the diffraction patterns. In addition to these ball-milled samples, a set of rehydrogenated samples was prepared in the following way. After ball-milling in H_2 atmosphere, a part of each sample was placed into a Sieverts-type apparatus for an additional dehydrogenation–hydrogenation cycle. Hydrogen was removed by heating the sample in vacuum up to 400 °C. The repeated hydrogenation was carried out at 300 °C and the hydrogen pressure of 1.2 MPa. This procedure leads to the increase in the fraction of the MgH_2 phase up to 95–97 wt.% and to the growth of the average grain size for this phase up to 50–60 nm.

NMR measurements were performed on a modernized Bruker SXP pulse spectrometer at the frequencies $\omega/2\pi = 14$, 23.8 and 90 MHz. The proton NMR spectra were recorded by Fourier transforming the spin echo signals. For the samples showing fast H motion, the $\pi/2$–τ–π pulse sequence was used, typical values of the delay τ being between 20 and 60 μs, and for the samples showing slow H motion, the $\pi/2$–τ–$\pi/2$ pulse sequence was used with $\tau = 14$ μs. For linewidths exceeding 70 kHz, the spectra were obtained by superimposing a number of Fourier spectra excited at different magnetic fields. The proton spin-lattice relaxation rates R_1 were measured using the saturation–recovery method.

3. Results and discussion

The measured proton spin-lattice relaxation rate R_1 in metal–hydrogen systems is usually determined by the sum of contributions resulting from the interactions of proton spins with conduction electrons (R_{1e}) and paramagnetic impurity ions (R_{1p}) and from the internuclear dipole–dipole interactions modulated by H motion (R_{1d}) [1]. The frequency-independent electronic (Korringa) contribution R_{1e} is typically proportional to the temperature, $R_{1e} = C_eT$. For most metallic systems, the electronic contribution dominates at low temperatures, while the motional contribution R_{1d} becomes more important in the temperature range where the H jump rate τ_d^{-1} is between 10^7 and 10^{11} s^{-1}. The temperature dependence of R_{1d} shows a characteristic peak at the temperature at which $\omega\tau_d \approx 1$. In the limit of slow H diffusion ($\omega\tau_d \gg 1$), R_{1d} is proportional to $\omega^{-2}\tau_d^{-1}$, and in the limit of fast H diffusion ($\omega\tau_d \ll 1$), R_{1d} is proportional to τ_d being frequency-independent. The behavior of the paramagnetic contribution R_{1p} is more complex; it depends on a number of parameters [12] including the spin-lattice relaxation time of paramagnetic ions τ_i.

3.1. Ball-milled Laves-phase hydrides $ZrCr_2H_3$

The temperature dependences of the proton spin-lattice relaxation rate measured at $\omega/2\pi = 14$ MHz in the coarse-grained and ball-milled samples of $ZrCr_2H_3$ are shown in Fig. 1. As can be seen from this figure, the ball milling leads to dramatic changes in the behavior of the relaxation rate. For all the samples studied, the relaxation rates are dominated by the sum of the contributions R_{1e} and R_{1d}. For the coarse-grained sample prepared by thermal hydrogenation the measured spin-lattice relaxation rate shows a peak near 200 K. The position of this peak related to the diffusive motion of hydrogen is consistent with the earlier results for polycrystalline $ZrCr_2H_x$ [13]. As the milling time increases, the amplitude of this peak rapidly decreases, and a new peak starts to grow near 370 K. In order to avoid structural relaxation and recrystallization of the nanostructured samples, we have not performed any measurements for them above 394 K; therefore, the high-temperature slope of the new peak is not observed. However, the frequency dependence of the spin-lattice relaxation rate indicates that this peak is also related to the diffusive motion of hydrogen. As an example of the data, Fig. 2 shows the measured proton spin-lattice relaxation rates at three frequencies for the sample milled for 10 h. The behavior of R_1 in the range 220–384 K is typical of that for the low-temperature slope of the relaxation rate peak due to H motion [1], although the frequency dependence of the relaxation rate in this range is somewhat weaker than ω^{-2}.

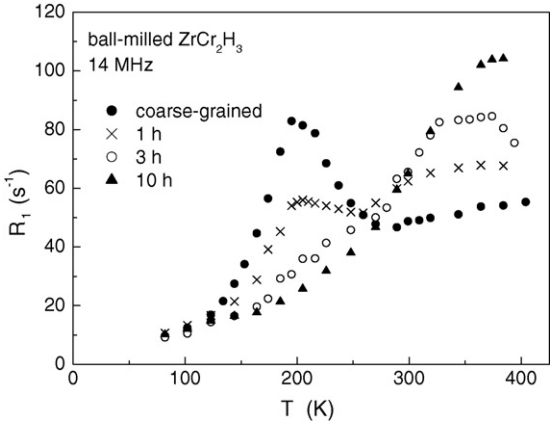

Fig. 1. The temperature dependences of the proton spin-lattice relaxation rates measured at 14 MHz for the coarse-grained $ZrCr_2H_3$ and for the nanostructured $ZrCr_2H_3$ systems prepared by ball milling for 1, 3 and 10 h.

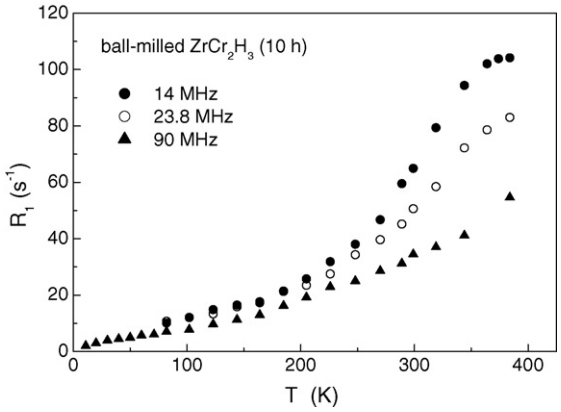

Fig. 2. The temperature dependences of the proton spin-lattice relaxation rates measured at 14, 23.8 and 90 MHz for the nanostructured $ZrCr_2H_3$ system prepared by ball milling for 10 h.

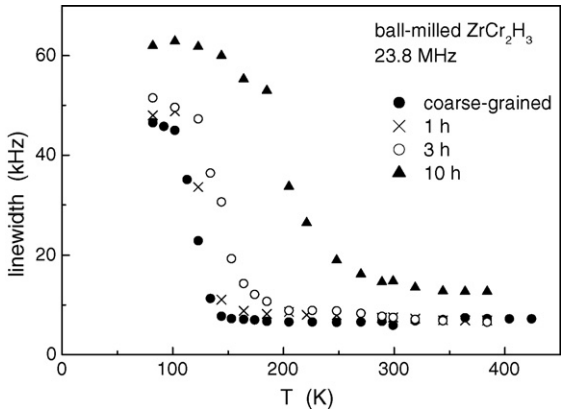

Fig. 3. The temperature dependences of the width (full width at half-maximum) of the proton NMR spectra measured at 23.8 MHz for the coarse-grained $ZrCr_2H_3$ and for the nanostructured $ZrCr_2H_3$ systems prepared by ball milling for 1, 3 and 10 h.

The observed shift of the R_1 peak position from ~200 to 370 K as a result of ball milling indicates the strong decrease in the H jump rate. For the samples with intermediate ball-milling times (1 and 3 h), both the low-temperature and high-temperature R_1 peaks appear to coexist. This suggests a coexistence of two H jump processes with different characteristic jump rates. It is natural to assume that the low-temperature R_1 peak originates from H motion in undistorted crystalline grains of $ZrCr_2H_x$. The volume fraction of these grains is expected to decrease with increasing milling time. The high-temperature R_1 peak can be attributed to H motion in strongly distorted intergrain regions; the corresponding H jump rate at a given temperature is much lower than that in undistorted grains. For the sample milled for 10 h, no signs of the R_1 peak due to H motion in undistorted grains can be found. It should be noted that in the entire temperature range studied the spin-lattice relaxation is well described by a single-exponential function. The single-exponential behavior of the spin-lattice relaxation in a system containing H atoms with different jump rates is expected to result from two mechanisms: the rapid exchange of H atoms between the grains and intergrain regions (above 200 K the corresponding exchange rate should be much higher than R_1) and the rapid equalization of spin polarization (*spin diffusion*) due to H–H dipole–dipole interaction.

Fig. 3 shows the temperature dependences of the ^{1}H NMR linewidth (full width at half-maximum) for the coarse-grained and ball-milled samples of $ZrCr_2H_x$. For all the samples studied, there is a range of sharp line narrowing. The narrowing becomes pronounced above the temperature at which the H jump rate exceeds the 'rigid-lattice' (low-temperature) linewidth [14]. Therefore, the observed shift of the T range of sharp line narrowing (Fig. 3) is consistent with the decrease in H mobility at long milling times. It is interesting to note that the comparison of the NMR data in the crystalline C15-type hydrides $ZrV_2H_x(D_x)$ and in amorphous hydrides of identical compositions [15] has also revealed a significant reduction of the hydrogen mobility in the amorphous samples. The opposite trend in the H mobility for most of the studied amorphous hydrides and their crystalline counterparts [16] is usually attributed to the fact that a structural disorder may give rise to the opening of new 'easy paths' for H diffusion. On the other hand, for Laves-phase hydrides the diffusion barriers are originally quite low, so that a structural disorder can only make the H diffusion more difficult. Similar arguments may be used for a qualitative interpretation of the decrease in H mobility resulting from ball milling of $ZrCr_2H_x$.

In the low-temperature region ($T \leq 82$ K) where the hydrogen diffusion is 'frozen out', the ^{1}H relaxation rates measured at 90 MHz are well described by the expression $R_1 = C_eT + B$ for all the samples studied. The Korringa coefficient C_e is found to decrease with the milling time, from 0.102 s^{-1} K^{-1} for the coarse-grained sample to 0.066 s^{-1} K^{-1} for the sample milled for 10 h. Since C_e is proportional to the square of the density of electron states at the Fermi level, $N^2(E_F)$ [14], the observed changes in C_e suggest that in the intergrain regions the value of $N(E_F)$ is lower than in $ZrCr_2H_3$ grains. The term B can be identified as the low-temperature limit of the paramagnetic contribution R_{1p} [12]. This term is found to increase with the milling time, from nearly zero for the coarse-grained sample to 1.6 s^{-1} for the sample milled for 10 h.

The value of the ^{1}H NMR linewidth at the high-temperature plateau (Fig. 3) is determined by a distribution of demagnetizing fields over the sample volume [14]. As can be seen from Fig. 3, the width of such a distribution for the sample milled for 10 h is larger than for the other samples studied. This broadening at long milling times may result from an increase in the number of paramagnetic centers appearing in the process of milling. Such a behavior is consistent with the increase in the term B of the low-temperature spin-lattice relaxation rate at long milling times.

3.2. Ball-milled MgH_2-based hydrides

The proton spin-lattice relaxation rate in the coarse-grained MgH_2 is very low. Our measurements at $\omega/2\pi = 23.8$ MHz have shown that at room temperature the value of R_1 in the MgH_2 prepared by thermal hydrogenation of Mg powder is 2.9×10^{-3} s^{-1}. This value can be compared to that reported for the coarse-grained MgH_2 earlier [17], $R_1 = 5 \times 10^{-3}$ s^{-1}. For

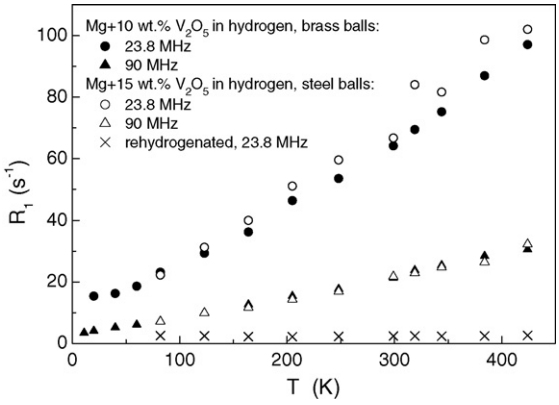

Fig. 4. The temperature dependences of the proton spin-lattice relaxation rates measured at 23.8 and 90 MHz for the nanostructured MgH_2 with V_2O_5. Solid symbols: Mg + 10 wt.% V_2O_5 milled in hydrogen with brass balls; open symbols: Mg + 15 wt.% V_2O_5 milled in hydrogen with steel balls; crosses: the same sample after rehydrogenation.

MgH_2 both the electronic (R_{1e}) and motional (R_{1d}) contributions to R_1 should vanish, since this hydride is non-metallic and the hydrogen mobility in it is extremely low. Therefore, the slow proton spin-lattice relaxation in MgH_2 appears to be quite natural. The main effect of ball milling on the proton spin-lattice relaxation rate in MgH_2-based hydrides is a strong enhancement of R_1. For all the ball-milled MgH_2-based samples studied, the measured relaxation rates are found to be several orders of magnitude higher than for the coarse-grained MgH_2.

As an example of the data, Fig. 4 shows the temperature dependences of R_1 for the nanocrystalline MgH_2 prepared by milling Mg + 15 wt.% V_2O_5 with steel balls and vial in hydrogen, the same sample after rehydrogenation, and the nanocrystalline MgH_2 prepared by milling Mg + 10 wt.% V_2O_5 with brass balls and vial in hydrogen. For the ball-milled samples the measured relaxation rate strongly depends on the temperature and resonance frequency. However, the observed behavior of R_1 in these samples cannot be ascribed to changes in the motional contribution R_{1d}. In fact, hydrogen motion with jump rates ${\tau_d}^{-1}$ exceeding $10^5\ s^{-1}$ would have led to considerable narrowing of the ^1H NMR line which has not been found for the MgH_2-based samples. For the sample prepared by milling Mg + 10 wt.% V_2O_5 with brass balls, the width of the ^1H NMR line at half-maximum does not show any changes in the temperature range 20–420 K, its value (~52 kHz) being typical of the 'rigid-lattice' linewidth due to dipole–dipole interactions between proton spins in concentrated hydrides. For the sample prepared by milling Mg + 15 wt.% V_2O_5 with steel balls, the observed ^1H NMR line is much broader (~290 kHz at $\omega/2\pi = 23.8$ MHz); this can be attributed to the strongly inhomogeneous magnetic field due to iron particles appearing in the process of milling. However, as can be seen from Fig. 4, the measured proton spin-lattice relaxation rates for the samples prepared by milling with brass and steel balls are nearly the same.

The most probable source of the R_1 enhancement for the ball-milled samples is the increase in the contribution R_{1p} due to interaction between proton spins and paramagnetic centers [12]. This is consistent with the observed frequency dependence of R_1 (see Fig. 4). Similar type of the frequency dependence of R_1 has been found for the other ball-milled MgH_2-based samples studied. As explained in Refs. [18,19], the paramagnetic contribution to the spin-lattice relaxation rate can be expressed in the approximate form,

$$R_{1p} = N\sigma \left[\frac{\tau_i}{1 + \omega^2 \tau_i^2} \right]^p, \quad (1)$$

where N is the concentration of paramagnetic centers, σ an adjustable parameter, and the exponent p can change from 1/4 (the strong collision regime) to 1 (the weak collision regime). Eq. (1) predicts a relaxation rate maximum corresponding to the condition $\omega\tau_i \approx 1$. It is evident that our experimental data should correspond to the region where $\omega\tau_i \gg 1$, and R_{1p} is expected to be proportional to ω^{-2p}. The ratio of the experimental R_1 values at $\omega/2\pi = 23.8$ and 90 MHz (Fig. 4) can be described with a nearly constant $p = 0.40$–0.44 over the temperature range 60–420 K.

It should be stressed that the paramagnetic centers which are believed to be responsible for the observed R_1 enhancement do not originate from the milling ball material; in other words, they cannot be considered as 'impurities'. In fact, the temperature and frequency dependences of R_1 for the samples prepared by milling with brass and steel balls appear to be nearly the same (Fig. 4). Furthermore, as can be seen from Fig. 4, the rehydrogenation of the ball-milled material results in the dramatic decrease in the proton relaxation rate. Similar strong reduction of R_1 after the rehydrogenation has been observed for all the samples studied. Since the rehydrogenation leads to the growth of the average grain size, it is likely that the paramagnetic centers appear on the surface of MgH_2 grains. However, the average grain size is not the only factor governing the R_1 enhancement. We have also found that the R_1 enhancement depends on the type and the physical state of the additives. Fig. 5 shows the temperature dependences of R_1 for the nanocrystalline MgH_2 prepared by milling Mg without any additives (steel balls) in hydrogen and the nanocrystalline MgH_2 prepared by milling

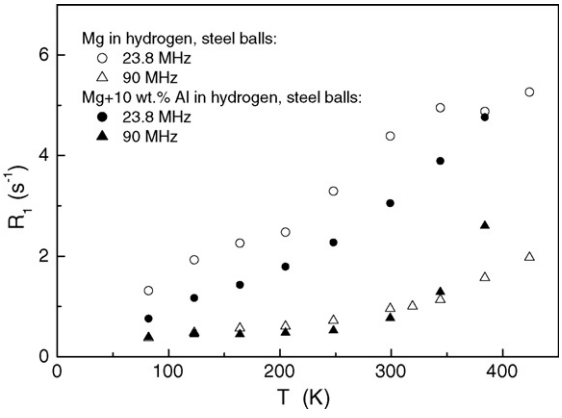

Fig. 5. The temperature dependences of the proton spin-lattice relaxation rates measured at 23.8 and 90 MHz for the nanostructured systems prepared by milling Mg in hydrogen with steel balls (open symbols) and by milling Mg + 10 wt.% Al in hydrogen with steel balls (solid symbols).

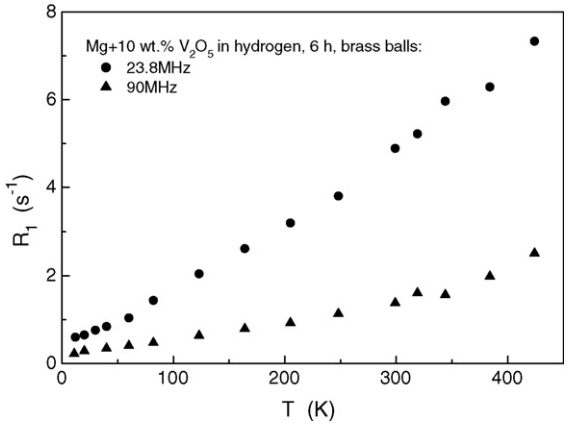

Fig. 6. The temperature dependences of the proton spin-lattice relaxation rates measured at 23.8 and 90 MHz for the nanostructured system prepared by milling Mg + 10 wt.% V_2O_5 for 6 h in hydrogen with brass balls.

Mg + 10 wt.% Al (steel balls) in hydrogen. Although the average grain size of the MgH_2 phase in these samples (12–15 nm) is the same as in the samples represented in Fig. 4, the measured proton spin-lattice relaxation rates for these samples are an order of magnitude lower (cf. Figs. 4 and 5). In order to study the importance of the average grain size somewhat further, we have prepared an additional sample by milling Mg + 10 wt.% V_2O_5 (brass balls) in hydrogen for 6 h. This sample can be considered as a 'not fully milled' counterpart of the samples represented in Fig. 4 and having $t_m \approx 20$ h. According to X-ray diffraction analysis, the average grain size of the MgH_2 phase in this sample is 13 nm; however, this sample contains about 60 wt.% of Mg and a small amount (~1 wt.%) of V_2O_5. Note that for the other ('fully milled') samples studied, no traces of V_2O_5 could be found in X-ray diffraction patterns. Fig. 6 shows the behavior of the proton spin-lattice relaxation rate for this 'not fully milled' sample. A comparison of Figs. 4 and 6 indicates that both the type of the temperature dependence of R_1 and the values of p describing the frequency dependency of R_1 for the 'fully milled' and 'not fully milled' samples are similar; however, the values of R_1 for the 'not fully milled' sample are an order of magnitude lower.

Summarizing the results of the proton spin-lattice relaxation rate measurements for the ball-milled MgH_2-based systems, we can conclude that the observed strong R_1 enhancement originates from the increase in the contribution due to interaction between proton spins and paramagnetic centers appearing in the process of milling. The R_1 enhancement is found to depend on the milling time and on the type of additives. The dramatic reduction of R_1 after the thermal rehydrogenation of the ball-milled samples suggests that the paramagnetic centers responsible for the R_1 enhancement are not just impurities originating from the milling tool material; these paramagnetic centers may result from broken bonds on the surface of MgH_2 grains. In particular, the chemical state of oxygen on the surface of the grains of a ball-milled material should differ from that in MgO [20]. This is expected to result from a very high density of structural defects on the surface of such grains, which gives rise to defects in the surface electronic structure [21]. It is not clear at present, whether these paramagnetic centers also play a significant role in catalytic activity responsible for the acceleration of hydrogenation kinetics. However, it is worth noting that, among the studied MgH_2-based samples, the sample with V_2O_5 additive having the highest proton spin-lattice relaxation rate shows the fastest hydrogenation kinetics [22].

4. Conclusions

The results of our proton NMR measurements for the ball-milled Laves-phase hydrides $ZrCr_2H_3$ indicate that the hydrogen mobility in this system strongly decreases with increasing milling time. The experimental data suggest that this effect is related to the growth of the fraction of highly distorted intergrain regions where H mobility is much lower than in the crystalline grains. These results are consistent with the previous data [15] for amorphous Laves-phase hydrides.

The main effect revealed for the ball-milled MgH_2-based systems is the strong enhancement of the proton spin-lattice relaxation rate R_1. For all the ball-milled samples studied, the measured relaxation rates are several orders of magnitude higher than for the coarse-grained MgH_2. The R_1 enhancement is found to depend on the milling time and the type of additives. While no effects of H jump motion on the proton NMR spectra have been found up to 420 K (this means that H jump rates remain below 10^5 s^{-1}), the observed R_1 enhancement can be attributed to the interaction between proton spins and paramagnetic centers appearing in the process of ball milling. As shown by experiments with different ball materials and with the thermal rehydrogenation of the ball-milled samples, these paramagnetic centers do not originate from the ball material. Most probably, the paramagnetic centers responsible for the R_1 enhancement result from broken bonds on the surface of MgH_2 grains.

Acknowledgements

This work was partially supported by the Russian Foundation for Basic Research (grant No. 06-02-16246) and by the Priority Program "Basic energy problems" of the Russian Academy of Sciences.

References

[1] R.G. Barnes, in: H. Wipf (Ed.), Hydrogen in Metals III, Springer, Berlin, 1997, p. 93.
[2] S. Orimo, F. Kimmerle, G. Majer, Phys. Rev. B 63 (2001) 094307.
[3] G. Majer, E. Stanik, S. Orimo, J. Alloys Compd. 356–357 (2003) 617.
[4] A.V. Skripov, Defect Diffus. Forum 224–225 (2003) 75.
[5] W. Renz, G. Majer, A.V. Skripov, A. Seeger, J. Phys.: Condens. Matter 6 (1994) 6367.
[6] Y. Chen, J.S. Williams, J. Alloys Compd. 217 (1995) 181.
[7] A. Zaluska, L. Zaluski, J.O. Ström-Olsen, J. Alloys Compd. 288 (1999) 217.
[8] G. Barkhordarian, T. Klassen, R. Bormann, J. Alloys Compd. 364 (2004) 242.
[9] Z. Luz, J. Genossar, P.S. Rudman, J. Less-Common Met. 73 (1980) 113.
[10] B. Vigeholm, J. Kjoller, B. Larsen, A.S. Pedersen, J. Less-Common Met. 89 (1983) 135.

[11] D. Fruchart, A. Rouault, C.B. Shoemaker, D.P. Shoemaker, J. Less-Common Met. 73 (1980) 363.
[12] T.T. Phua, B.J. Beaudry, D.T. Peterson, D.R. Torgeson, R.G. Barnes, M. Belhoul, G.A. Styles, E.F.W. Seymour, Phys. Rev. B 28 (1983) 6227.
[13] A.V. Skripov, M.Yu. Belyaev, A.P. Stepanov, Solid State Commun. 78 (1991) 909.
[14] R.M. Cotts, in: G. Alefeld, J. Völkl (Eds.), Hydrogen in Metals I, Springer, Berlin, 1978, p. 227.
[15] S.V. Rychkova, M.Yu. Belyaev, A.V. Skripov, A.P. Stepanov, Sov. Phys. Solid State 30 (1988) 1285.
[16] D. Richter, R. Hempelmann, R.C. Bowman, in: L. Schlapbach (Ed.), Hydrogen in Intermetallic Compounds II, Springer, Berlin, 1992, p. 97.
[17] M. Stioui, A. Grayevsky, A. Moran, S. Kreitzman, N. Kaplan, D. Shaltiel, J. Less-Common Met. 104 (1984) 119.
[18] E. Fukushima, E.A. Uehling, Phys. Rev. 173 (1968) 366.
[19] S. Leyer, R.G. Barnes, C. Buschhaus, G. Fischer, B. Pilawa, B. Pongs, A. Tinner, E. Dormann, J. Phys.: Condens. Matter 16 (2004) 6147.
[20] I.G. Konstanchuk, E.Yu. Ivanov, V.V. Boldyrev, Russ. Chem. Rev. 67 (1998) 69.
[21] V. Henrich, Rep. Prog. Phys. 48 (1985) 1481.
[22] A.Ye. Yermakov, N.V. Mushnikov, M.A. Uimin, V.S. Gaviko, A.P. Tankeyev, A.V. Skripov, A.V. Soloninin, A.L. Buzlukov, J. Alloys Compd. 425 (2006) 367.